nature photonics

LETTERS

PUBLISHED ONLINE: 19 DECEMBER 2010 | DOI: 10.1038/NPHOTON.2010.286

Lasing oscillation in a three-dimensional photonic crystal nanocavity with a complete bandgap

Aniwat Tandaechanurat*, Satomi Ishida, Denis Guimard, Masahiro Nomura, Satoshi Iwamoto and Yasuhiko Arakawa*

Photonic crystals[1,2] have been extensively used in the control and manipulation of photons in engineered electromagnetic environments provided by means of photonic bandgap effects. These effects are key to realizing future optoelectronic devices, including highly efficient lasers. To date, lasers based on photonic crystal cavities have been exclusively demonstrated in two-dimensional photonic crystal geometries[3–6]. However, full confinement of photons and control of their interaction with materials can only be achieved with the use of three-dimensional photonic crystals with complete photonic bandgaps[7–16]. We demonstrate, for the first time, the realization of lasing oscillation in a three-dimensional photonic crystal nanocavity. The laser is constructed by coupling a cavity mode exhibiting the highest quality factor yet achieved (∼38,500) with quantum dots. This achievement provides means for exploring the physics of light–matter interactions in a nanocavity–single quantum dot coupling system in which both photons and electrons are confined in three dimensions, as well as for realizing three-dimensional integrated photonic circuits.

Three-dimensional photonic crystals have the facility to inhibit light propagation in any direction by means of their complete photonic bandgaps (PBGs). By introducing an artificial defect into a perfect crystal, three-dimensional photonic-crystal nanocavity modes with high quality (Q) factors and small mode volumes (of the order of a cubic wavelength) can be localized in a complete PBG, a feature that is essential for achieving ultimate control of light–matter interactions. Three-dimensional photonic crystals also offer the possibility of directly funnelling the light output from the cavity[17] and subsequently guiding it through optical circuit paths to other optical devices on the same chip with low loss[8,13]. Furthermore, three-dimensional photonic crystals can also be made to couple with material with gain polarized in any direction as a result of the omnidirectional property of the complete PBG[1,18]. Despite these striking advantages, the realization of three-dimensional photonic crystal lasers has been hindered by difficulties in fabricating intricate three-dimensional structures that have a complete PBG and contain a high-Q cavity incorporating an efficient light-emitting material. Lasing in three-dimensional photonic crystal structures has previously been attempted using a pseudo-gap[19–22], but not a complete PBG. It would be difficult to use such structures to gain the abovementioned advantages because they can manipulate photons only in a specific direction. Although several efforts have been devoted to improving the quality of active cavities embedded in complete-PBG crystals[14–16], lasing oscillation has yet to be realized because of relatively low Q factors and/or insufficient material gain. In this Letter, we report the first demonstration of a three-dimensional photonic crystal nanocavity laser under pulsed operation at low temperature, by coupling a high-Q cavity mode, which is localized in a complete PBG and has a record Q factor of 38,500, with high-quality InAs quantum dots[23]. We also demonstrate a systematic change in the laser characteristics, including the threshold and spontaneous emission coupling factor (β), by controlling the crystal size, which consequently changes the strength of photon confinement in the third dimension.

A schematic representation of the fabricated three-dimensional photonic crystal, a so-called woodpile structure, is shown in Fig. 1a. The structure comprises a stack of GaAs-based two-dimensional thin layers, each containing a line-and-space pattern with 11 in-plane (x–y plane) rods fabricated using micromanipulation techniques[15,16]. An active layer embedding a point-defect structure (dimensions, 1.15 μm × 1.15 μm) and three-layer stacked InAs quantum-dot layers (see Fig. 1b) with a dot density of $\sim 4 \times 10^{10}$ cm^{-2} per layer (as cavity and light emitter, respectively) was sandwiched between the upper and lower layers. The quantum dot ground-state emission peak was at 1.26 μm at 7 K. The in-plane periodicity, thickness and width of the rods of each layer, including the active layer, were set at 500 nm, 150 nm and 130 nm, respectively. The number of lower layers of the structure was set at 12, and the number of upper layers increased from an initial value of 2 to 12. Scanning electron microscopy (SEM) images of the fabricated structure are shown in Fig. 1c. The rectangular posts that can be observed in the image help to guide the layers to a designated position, allowing high-precision assembly with a stacking error of less than 50 nm. The fabrication time required for assembling one layer was less than 10 min. Details of the fabrication process are provided in the Methods.

As further upper layers were stacked onto the structure, photoluminescence measurements were performed at 7 K. We initially investigated the effect of the number of upper layers on the Q factor of a high-Q cavity mode. Figure 2a shows the photoluminescence spectrum for the structure with six upper layers, which demonstrates a number of cavity modes in a complete PBG between 1,085 and 1,335 nm, predicted by calculations using a plane-wave expansion (PWE) method. The Q factor of the mode with the most pronounced intensity at ∼1,200 nm, very close to the centre wavelength of the PBG where the localization of photons was the strongest[16], is plotted as a function of the number of upper layers in Fig. 2b. We estimated the value of the measured Q from a Lorentzian fit to the experimental data measured at the transparency pump power. The Q factor grew exponentially with the number of upper layers as a result of the strengthening of the PBG effect[24], reaching a value of 38,500 (Fig. 2c) for the structure with 12 upper layers. This is the highest Q value reported to date for three-dimensional photonic crystal nanocavities. These results agreed well with theoretical calculations. In addition to

Institute for Nano Quantum Information Electronics, The University of Tokyo, 4-6-1 Komaba, Meguro, Tokyo 153-8505, Japan. *e-mail: aniwat@iis.u-tokyo.ac.jp; arakawa@iis.u-tokyo.ac.jp

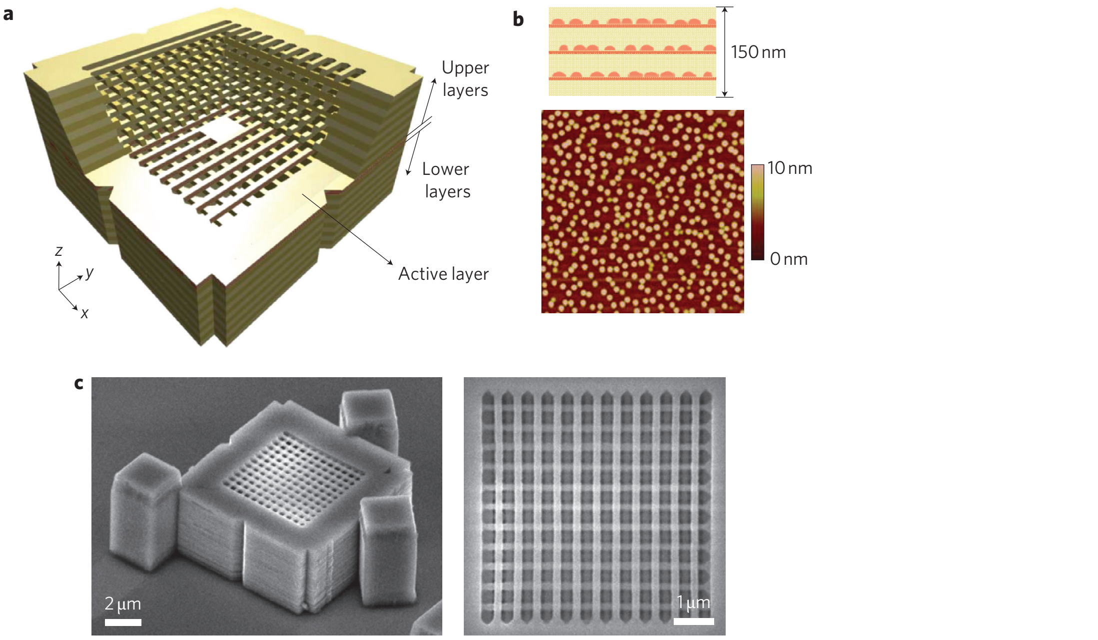

Figure 1 | Three-dimensional photonic crystal laser structure. a, Schematic of a fabricated three-dimensional photonic crystal. A portion of the upper layers is removed to show the cross-section of the stacked structure and to reveal the cavity structure. **b**, Illustration of a cross-section of an active layer showing three-layer stacked quantum dots (upper). Also shown (lower) is a $1 \times 1\ \mu m^2$ planar atomic force microscope image of InAs quantum dots on a GaAs matrix. **c**, SEM images of the fabricated 25-layer woodpile structure shown in bird's eye (left) and top (right) views.

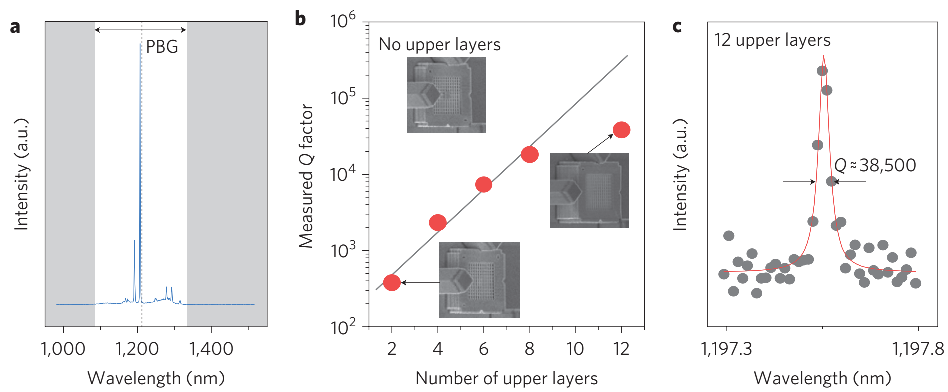

Figure 2 | High-*Q* nanocavity mode. a, Photoluminescence spectrum for the structure with six upper layers pumped with a c.w. Ti:sapphire laser. The complete PBG is shown as an unshaded area. A dotted line represents the centre wavelength of the PBG. **b**, Dependence of the measured *Q* factor of the mode at 1,200 nm on the number of upper layers. The line is the exponential fit. Insets: SEM images of the fabricated structures with the corresponding number of upper layers. **c**, High-resolution photoluminescence spectrum fitted with a Lorentzian function for the structure with 12 upper layers, exhibiting the highest *Q* factor achieved to date, ~38,500.

achieving the highest *Q* factor, these results also present experimental evidence confirming direct control of photon confinement in the third dimension. The growth in *Q* began to saturate when the number of upper layers was more than eight, approaching a limit mainly determined by the small size of the photonic crystal in the in-plane direction. Increasing the number of rods in the in-plane direction could therefore further improve the *Q* factor (see Supplementary Information).

Pulsed operation of the three-dimensional photonic crystal lasers was achieved when the number of upper layers was six or more. The structure was pumped by 8 ns pulses at a wavelength of 905 nm from a semiconductor laser with a repetition rate of 25 kHz. Figure 3 shows the output power of the lasing mode as a function of pump power (*L*–*L* plot) for structures with different numbers of upper layers. With four upper layers, it is clear that no lasing oscillation has occurred in the structure because of its low *Q* value resulting from a weak three-dimensional confinement effect. The lasing spectrum for each of the other laser structures (pumped at a peak pulse power of 150 mW) is shown in the inset. Lasing thresholds were obtained by extrapolating the plots back from above threshold to zero output power. The lasing threshold was reduced from 12 mW to 10 mW and 6.5 mW peak pulse power when the number of upper layers was increased from 6 to 8 and 12, respectively, which could be attributed to the improvement in *Q*. The narrowing of the emission linewidth of the lasing mode, being evidence of lasing, was also observed (see Supplementary Information). We simulated the values of the threshold power as a function of *Q* factor using coupled rate equations for the carrier density and photon density[25]. The general trend for the simulated threshold power was in good agreement with experimental values,

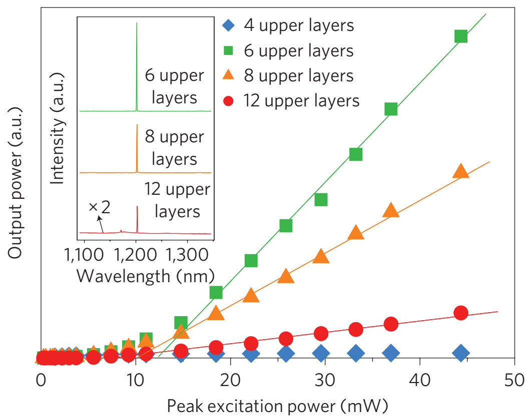

Figure 3 | Lasing oscillation and its threshold characteristics. *L–L* plots for structures with different numbers of upper layers. Lines are the linear fits for the experimental plots above threshold. Inset: lasing spectra for each structure pumped at a peak pulse power of 150 mW. With four upper layers, lasing oscillation was not observed.

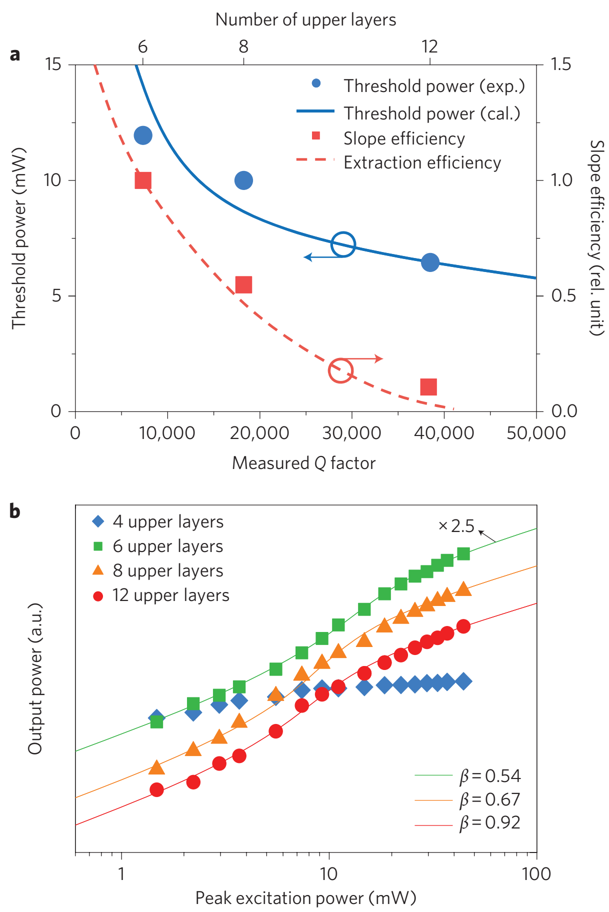

Figure 4 | Effects of number of upper layers on laser characteristics. **a**, Threshold power (blue circles) and laser slope efficiency (red squares) as a function of *Q* factor. *Q* factors are 7,400, 18,300 and 38,500 for the structures with 6, 8 and 12 upper layers, respectively (see also Fig. 2b). Also plotted is the simulated threshold power (solid curve) calculated using rate equations, and the light extraction efficiency (dashed curve) as a function of *Q* factor. **b**, Experimental *L–L* plots (symbols) and fitting curves obtained from rate equation analysis with best-fitted values of β. The plot and curve for the structure with six upper layers have been shifted upwards for clarity. The *L–L* plot for the non-lasing structure with four upper layers is also shown for comparison.

as shown in Fig. 4a. In addition, we also observed a reduction in laser slope efficiency, where light output radiating out from the cavity into the top side of the structure was more strongly suppressed as more upper layers were added, consistent with the extraction efficiency calculated by comparing the cavity loss rate into the top side with the total loss rate defined as the sum of the cavity loss rate into all directions and the scattering loss rate due to fabrication imperfections. We then evaluated the value of the spontaneous emission coupling factor β, which is a measure of the coupling efficiency of the spontaneous emission to the lasing mode. Because of the existence of the complete PBG in the present laser, where the lasing mode was strongly confined and well isolated from other leaky optical modes, a high value of β was expected. Fitting the experimental *L–L* plots with steady-state solutions of the rate equations on double logarithmic scales as shown in Fig. 4b, we determined β values of 0.54, 0.67 and 0.92 for the laser structures with 6, 8 and 12 upper layers, respectively. For the structure with 12 upper layers, the value of β was very close to the theoretical limit of unity[26] (when analysed with this simple rate equation model, at least), which can be attributed to the very high *Q* factor of the lasing mode localized in the complete PBG. Finally, we note that the *L–L* plot for the non-lasing structure with four upper layers shows no nonlinear S-shaped behaviour, indicating that it was not lased.

We have demonstrated lasing oscillation in a three-dimensional photonic crystal nanocavity by coupling a high-*Q* cavity mode with quantum dots. Localizing the lasing mode in a complete PBG allowed us to strongly confine light in the cavity and effectively restrict undesired spontaneous emission, as was evident from the high cavity *Q* and high β factor, respectively. We believe that our demonstration of lasers in three-dimensional photonic crystals should significantly advance the development of practical three-dimensional integrated photonic circuits, as the light source has now been provided. Furthermore, introducing a single quantum dot into the present high-*Q* three-dimensional photonic crystal nanocavity would establish an ideal solid-state system for the study of the light–matter interaction between three-dimensionally confined photons and electrons enclosed in a completely engineered electromagnetic environment. This may lead us to the discovery of new physics in the field of cavity quantum electrodynamics.

Methods

The 150-nm-thick GaAs layers used for the fabrication of the three-dimensional photonic crystal were grown on a 1,000-nm-thick $Al_{0.7}Ga_{0.3}As$ sacrificial layer using metal–organic chemical vapour deposition. Line-and-space patterns were formed using an electron-beam lithography system and then transferred through the GaAs slab by inductively coupled plasma reactive ion etching. The sacrificial layer was removed by a wet-etching process using a dilute hydrogen fluoride solution to form air-bridge structures. An active layer was prepared in the same way as the GaAs layers, but contained three-layer stacked InAs quantum dot layers in which the middle quantum dot layer was at the centre of the slab. These GaAs layers were stacked to construct the three-dimensional structure using a micromanipulation system installed in an SEM chamber[15,16]. The nanocavity was designed so that the resonance of the lasing mode was located as close as possible to the centre wavelength of the PBG. Properties of the cavity resonance such as resonant wavelength and *Q* factor were calculated using a three-dimensional finite-difference time-domain (FDTD) method. The dimensions of the simulated structures were set to be identical to those of the fabricated structures.

Photoluminescence measurements were performed in a temperature-controlled liquid-helium cryostat at 7 K. The structure was optically pumped by a continuous-wave (c.w.) Ti:sapphire laser or by a pulsed semiconductor laser with a focal spot of ~4 μm with a ×40 objective lens (numerical aperture, NA = 0.6). Both lasers were operated at 905 nm. The photoluminescence spectra were recorded using a spectrometer with a spectral resolution of ~0.02 nm and an InGaAs photodiode array. After the spectra were collected, the sample was removed from the cryostat so that additional upper layers could be added onto the structure. Another set of measurements was then performed. These procedures were repeated until the number of upper layers reached 12.

Received 27 April 2010; accepted 15 November 2010; published online 19 December 2010

References

1. Yablonovitch, E. Inhibited spontaneous emission in solid-state physics and electronics. *Phys. Rev. Lett.* **58,** 2059–2062 (1987).
2. John, S. Strong localization of photons in certain disordered dielectric superlattices. *Phys. Rev. Lett.* **58,** 2486–2489 (1987).
3. Painter, O. *et al.* Two-dimensional photonic band-gap defect mode laser. *Science* **284,** 1819–1821 (1999).
4. Strauf, S. *et al.* Self-tuned quantum dot gain in photonic crystal lasers. *Phys. Rev. Lett.* **96,** 127404 (2006).
5. Nomura, M., Kumagai, N., Iwamoto, S., Ota, Y. & Arakawa, Y. Laser oscillation in a strongly coupled single-quantum-dot–nanocavity system. *Nature Phys.* **6,** 279–283 (2010).
6. Altug, H., Englund, D. & Vučković, J. Ultrafast photonic crystal nanocavity laser. *Nature Phys.* **2,** 484–488 (2006).
7. Lin, S. Y. *et al.* A three-dimensional photonic crystal operating at infrared wavelengths. *Nature* **394,** 251–253 (1998).
8. Noda, S., Tomoda, K., Yamamoto, N. & Chutinan, A. Full three-dimensional photonic bandgap crystals at near-infrared wavelengths. *Science* **289,** 604–606 (2000).
9. Deubel, M. *et al.* Direct laser writing of three-dimensional photonic-crystal templates for telecommunications. *Nature Mater.* **3,** 444–447 (2004).
10. Takahashi, S. *et al.* Direct creation of three-dimensional photonic crystals by a top-down approach. *Nature Mater.* **8,** 721–725 (2009).
11. Qi, M. H. *et al.* A three-dimensional optical photonic crystal with designed point defects. *Nature* **429,** 538–542 (2004).
12. Blanco, A. *et al.* Large-scale synthesis of a silicon photonic crystal with a complete three-dimensional bandgap near 1.5 micrometers. *Nature* **405,** 437–440 (2000).
13. Rinne, S. A., García-Santamaría, F. & Braun, P. V. Embedded cavities and waveguides in three-dimensional silicon photonic crystals. *Nature Photon.* **2,** 52–56 (2008).
14. Ogawa, S., Imada, M., Yoshimoto, S., Okano, M. & Noda, S. Control of light emission by 3D photonic crystals. *Science* **305,** 227–229 (2004).
15. Aoki, K. *et al.* Coupling of quantum-dot light emission with a three-dimensional photonic-crystal nanocavity. *Nature Photon.* **2,** 688–692 (2008).
16. Tandaechanurat, A. *et al.* Demonstration of high-Q (>8600) three-dimensional photonic crystal nanocavity embedding quantum dots. *Appl. Phys. Lett.* **94,** 171115 (2009).
17. Okano, M., Kako, S. & Noda, S. Coupling between a point-defect cavity and a line-defect waveguide in three-dimensional photonic crystal. *Phys. Rev. B* **68,** 235110 (2003).
18. Ho, K. M., Chan, C. T. & Soukoulis, C. M. Existence of a photonic gap in periodic dielectric structures. *Phys. Rev. Lett.* **65,** 3152–3155 (1990).
19. Cao, W., Muñoz, A., Palffy-Muhoray, P. & Taheri, B. Lasing in a three-dimensional photonic crystal of the liquid crystal blue phase II. *Nature Mater.* **1,** 111–113 (2002).
20. Lin, H. Y. *et al.* Laser action in $Tb(OH)_3/SiO_2$ photonic crystals. *Opt. Express* **16,** 16697–16703 (2008).
21. Scharrer, M., Yamilov, A., Wu, X., Cao, H. & Chang, R. P. H. Ultraviolet lasing in high-order bands of three-dimensional ZnO photonic crystals. *Appl. Phys. Lett.* **88,** 201103 (2006).
22. Shkunov, M. N. *et al.* Tunable, gap-state lasing in switchable directions for opal photonic crystals. *Adv. Funct. Mater.* **12,** 21–26 (2002).
23. Guimard, D. *et al.* Interface properties of InAs quantum dots produced by antimony surfactant-mediated growth: etching of segregated antimony and its impact on the photoluminescence and lasing characteristics. *Appl. Phys. Lett.* **94,** 103116 (2009).
24. Villeneuve, P. R., Fan, S. & Joannopoulos, J. D. Microcavities in photonic crystals: mode symmetry, tunability, and coupling efficiency. *Phys. Rev. B* **54,** 7837–7842 (1996).
25. Coldren, L. A. & Corzine, S. W. *Diode Lasers and Photonic Integrated Circuits* (Wiley, 1995).
26. Björk, G. & Yamamoto, Y. Analysis of semiconductor microcavity lasers using rate equations. *IEEE J. Quantum Electron.* **27,** 2386–2396 (1991).

Acknowledgements

The authors thank D. Bordel, M. Nishioka, L. Jalabert and K. Aoki for their technical support. This work was supported by the Special Coordination Funds for Promoting Science and Technology.

Author contributions

A.T. developed the device design and conducted the theoretical simulations and analysis of data. A.T. and S. Ishida fabricated the device. D.G. carried out the semiconductor growth. A.T. and M.N. performed the optical measurements. Y.A. and S. Iwamoto planned the research and supervised the experiment. A.T., M.N., S. Iwamoto and Y.A. wrote the manuscript. All authors contributed to the discussion of the results.

Additional information

The authors declare no competing financial interests. Supplementary information accompanies this paper at www.nature.com/naturephotonics. Reprints and permission information is available online at http://npg.nature.com/reprintsandpermissions/. Correspondence and requests for materials should be addressed to A.T. and Y.A.